Antiviral Research 87 (2010) 57–66

Contents lists available at ScienceDirect

Antiviral Research

journal homepage: www.elsevier.com/locate/antiviral

Monitoring hepatitis C virus (HCV) RNA-dependent RNA polymerase oligomerization by a FRET-based *in vitro* system

Itxaso Bellón-Echeverría, Alberto José López-Jiménez, Pilar Clemente-Casares, Antonio Mas*

Centro Regional de Investigaciones Biomédicas (CRIB), Universidad de Castilla-La Mancha, C/Almansa 14, 02006 Albacete, Spain

ARTICLE INFO

Article history:
Received 25 February 2010
Received in revised form 15 April 2010
Accepted 19 April 2010

Keywords:
RNA polymerase
HCV
Oligomerization
Inhibitors
FRET

ABSTRACT

Hepatitis C virus (HCV) is a positive-strand RNA virus ((+)RNA) that replicates its genome in replication complexes (RC) associated to endoplasmic reticulum (ER)-derived micro-vesicles. One key protein in these complexes is NS5B, a viral enzyme that shows the RNA binding and RNA-dependent RNA polymerase (RdRp) activities. For this reason, NS5B protein has become one of the most important targets for designing new antiviral therapy compounds. Recently, it has been demonstrated that NS5B interacts itself forming oligomers, and mutations that disrupt these interactions are lethal for polymerase function. Therefore, NS5B oligomerization could be a new target for the design of anti-HCV compounds. In this study we describe a new accurate method to analyze NS5B–NS5B interactions by using Förster-resonance-energy transfer (FRET). This method allows analyses of the conditions, mainly ionic strength, driving the interactions between NS5B-cyan and NS5B-citrine constructs. Experiments using different combinations of point mutants rendered FRET values from zero to around 100%, suggesting the geometry of the interaction. Finally, oligomerization experiments in the presence of non-nucleoside inhibitor (NNI) PF-254027 gave a statistically significant reduction in the FRET signal, suggesting a new connection between NS5B oligomerization and NNI binding.

1. Introduction

Hepatitis C virus (HCV) is a member of the Flaviviridae family of viruses, and it infects about 3% of the human population worldwide. HCV infection frequently leads to chronic hepatitis, liver cirrhosis, and eventually hepatocellular carcinoma. Taking into consideration the population affected and the induced disease, HCV ranks as one of the most important human pathogens (Lavanchy, 2008). The HCV genome consists of a positive-sense, single-stranded RNA of approximately 9.6 kb which encodes a large open reading frame flanked by untranslated regions at both the 5′ and the 3′ ends. HCV RNA translation produces a polyprotein of approximately 3000 amino acids that is processed by host and viral proteases into mature structural (C, E1 and E2) and non-structural proteins (p7, NS2, NS3, NS4A, NS4B, NS5A, NS5B). From these proteins, non-structural protein 5B (NS5B) contains the GDD signature motif and enzymatic activity typical of an RNA-dependent RNA polymerase (RdRp) (Behrens et al., 1996; Lohmann et al., 1997). The essentiality of the NS5B protein has been established in a chimpanzee model (Kolykhalov et al., 2000), and therefore, NS5B is currently one of the main targets for the design of anti-HCV compounds (De Francesco and Migliaccio, 2005; Webster et al., 2009).

Positive-strand RNA ((+)RNA) viruses need cellular membranes to localize viral and cellular proteins necessary for viral replication (Caliguiri and Tamm, 1969; Sreevalsan, 1970; Ralph et al., 1971; Allison, 1971). Recently, description of (+)RNA virus replication complexes (RCs) at a molecular level has been approached with animal (Westaway et al., 1997; Magliano et al., 1998; Kujala et al., 2001; Gosert et al., 2002; Schwartz et al., 2002; Kopek et al., 2007; Miller and Krijnse-Locker, 2008; Welsch et al., 2009) and plant viruses (Prod'homme et al., 2001; Kim, 1977; Hatta and Francki, 1981; Carette et al., 2002). The cellular origin of the membranes in RCs can vary from one virus to another. Viral replication can occur in membranes of endosomes, lysosomes, autophagosomal pathway, mitochondria although, most common, lipidic membranes are recruited from endoplasmic reticulum (ER) and Golgi apparatus (Taylor and Kirkegaard, 2008; reviewed in Denison, 2008). HCV is not an exception and viral RCs have been described associated with ER-derived membranes (Egger et al., 2002; Gosert et al., 2003).

Recently, Quinkert et al. (2005) detected a great excess of each HCV non-structural protein respect to positive- and negative-sense HCV RNAs in the ER-derived micro-vesicles. Kopek and co-workers showed similar results working with flock-house virus (FHV) (Kopek et al., 2007). From these data, extensive protein–protein interactions and molecular crowding phenomena must occur inside these vesicles. In this context, interactions between HCV proteins NS5A and NS5B, and between NS5A, NS5B and cellular proteins have been previously demonstrated (Qin et al., 2001; Shirota

* Corresponding author. Tel.: +34 967 599 200; fax: +34 967 599 360.
E-mail address: Antonio.Mas@uclm.es (A. Mas).

0166-3542/$ – see front matter © 2010 Elsevier B.V. All rights reserved.
doi:10.1016/j.antiviral.2010.04.009

et al., 2002; Shimakami et al., 2004; Tu et al., 1999; Choi et al., 2004; Gao et al., 2004). Moreover, HCV NS5B interacts with itself and these homotypic interactions may be critical for polymerase activity (Wang et al., 2002; Qin et al., 2002; Gu et al., 2004), as also described previously for poliovirus RdRp (Pata et al., 1995; Lyle et al., 2002; Hobson et al., 2001). Furthermore, it has been suggested that oligomerization could be the target for some non-nucleoside inhibitors directed against NS5B protein (Love et al., 2003; Wang et al., 2003; Biswal et al., 2006). Conditions that regulate NS5B oligomerization may include ionic strength, since NS5B monomers have been observed only at NaCl concentrations above 300 mM (Cramer et al., 2006).

Förster-resonance-energy transfer (FRET) is a mechanism describing energy transfer between two chromophores. Briefly, a donor chromophore, initially in its electronic excited state, may transfer energy to an acceptor chromophore through nonradiative dipole–dipole coupling. The FRET efficiency depends on the distance between the donor and the acceptor chromophores, the spectral overlap between the donor emission spectrum and the acceptor absorption spectrum, and the relative orientations of the donor emission moment and the acceptor absorption dipole moments (Förster, 1965). Nowadays, a large set of compounds with different fluorescent properties is available. Proteins derived from the green fluorescent protein (GFP) are the most representative ones. From them, enhanced-cyan-fluorescent protein (ECFP or cyan) and citrine are the most popular pair of proteins for FRET analyses due to their fluorescent properties, including overlapping excitation and emission spectra, and brightness. Förster radius for this pair of proteins is ~49 Å (Patterson et al., 2000), and therefore, FRET occurs when both chromophores are in closed proximity (10 nm or less). This is the main reason why FRET-based methods have become a gold-standard to analyze protein–protein interactions both *in vivo* and *in vitro* (Miyawaki and Tsien, 2000).

In the present study, we have developed a new fluorescence-based method to study quantitatively the HCV NS5B–NS5B interactions. In our assay (Fig. 1A), we detect FRET when energy is transferred from the fusion protein NS5BΔ55-cyan to its counterpart NS5BΔ55-citrine, observing citrine fluorescence emission when exciting the sample at the excitation wavelength for cyan. This assay has allowed us to (i) define quantitatively the conditions needed to go from monomeric to oligomeric states, (ii) delineate the overall structure of the oligomers, (iii) determine the activity of molecules capable of disrupting these NS5B–NS5B interactions, and (iv) connect non-nucleoside inhibitor binding with interference with NS5B oligomerization.

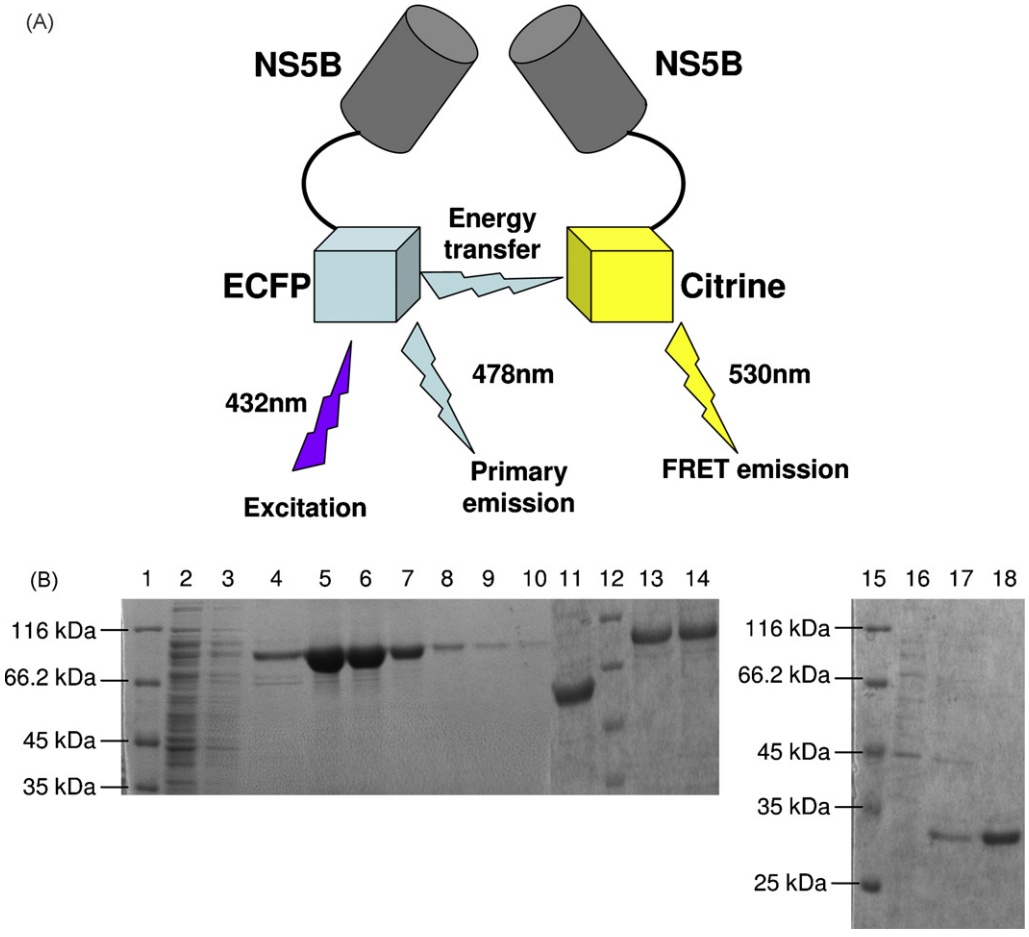

Fig. 1. (A) Experimental design. Schematic representation of the FRET assay for the analysis of NS5B–NS5B interactions. NS5B HCV polymerase (gray) is fused either to cyan (in cyan) or to citrine (in yellow). If NS5B–NS5B interactions occur, and the distance and orientation between cyan and citrine are correct, excitation of cyan at 432 nm produces its emission of energy with a peak at 475 nm. Part of this energy is captured as primary emission and the rest is transferred to citrine (energy transfer) that, in turn, emits with a peak at 530 nm (FRET emission). (B) Proteins used in the FRET assays. Lanes 1–10 correspond to aliquots of material obtained from each step during fusion protein purification were resolved in a 10% SDS-PAGE. Lane 1: molecular weight markers; lane 2: flow-through; lane 3: 20 mM imidazol washing step; lane 4: 40 mM imidazol washing step; lanes 5–10: fractions eluted by 250 mM imidazol. Lanes 11–14 correspond to a comparison of purified NS5BΔ55 with purified NS5B fused to fluorescence proteins; lane 11, NS5BΔ55; lane 12, molecular weight marker; lane 13, NS5BΔ55-cyan; lane 14, NS5BΔ55-citrine. Lanes 15–18 correspond to a typical citrine purification procedure resolved in a 12% SDS-PAGE. Lane 15, molecular weight markers; lane 16, flow-through; lane 17: 20 mM imidazol wash step; lane 18: products eluted by 50 mM imidazol. (For interpretation of the references to color in this figure legend, the reader is referred to the web version of the article.).

2. Materials and methods

2.1. HCV NS5B polymerase, fluorescent proteins, and plasmid constructs

NS5BΔ55 mutant from BK strain and the coding regions for fluorescent proteins (FP) named enhanced-cyan-fluorescent protein (ECFP or cyan) and citrine were obtained by PCR from plasmids pDest14-NS5B1b-WT, pcDNA3-cyan, and pRSET-citrine, respectively. Aequorea fluorescent proteins tend to dimerize, and dimers of fluorescent proteins can overwhelm detection of true NS5B–NS5B interactions. For this reason, we selected nondimerizing cyan and citrine variants of Aequorea green fluorescent protein for our assay, and both variants carry the A206K mutation that prevents fluorescence protein dimerization (Zacharias et al., 2002). We used NS5B with a deletion of 55 amino acids in its C-terminal because it allows solubilization of the recombinant protein. PCR amplification was carried out using the primers described in Table 1 designed for cloning by Gateway technology (Invitrogen). Briefly, the sequence coding for NS5BΔ55 was amplified by using the sense primer ATTB1_NS5B that includes the AttB1 sequence, the ATG for translation initiation, and an extra Lys codon AAA that enhances translation (Care et al., 2008). The antisense primer was NS5B_5G (Table 1) that includes a linker sequence consisting on five glycines and the sequence encoding for the first eight amino acids of the fluorescent protein. The sequences coding for citrine or cyan were amplified using the sense primer FPs_5G, which includes the last eight amino acids of NS5BΔ55 and the linker sequence for five glycines, and the antisense primer FPs_ATTB2, which includes sequences encoding for a 6xHis tag, the stop codon, and the AttB2 site (Table 1). Following this strategy, we obtained the coding sequence for NS5BΔ55 with a 3′ end tail encoding the glycine linker and the first eight amino acids of the fluorescent protein, as well as the coding sequence for the fluorescence protein, with a 5′ tail sequence encoding the last eight amino acids of the NS5BΔ55 and the glycine linker. The final Nt-NS5BΔ55-linker-FP-6xHis-Ct fusion DNA was obtained by PCR using as templates the required PCR products, and the sense and antisense primers ATTB1_NS5B and FPs_ATTB2, respectively (Table 1). All PCR reactions were performed using a high-fidelity polymerase (Expand High Fidelity System, Roche). PCR products containing NS5B-FP fusions were cloned into the pDest14 vector by using the Gateway technology to obtain the final pDest14-NS5BΔ55-FP constructs (NS5BΔ55-cyan and NS5BΔ55-citrine). Point mutants were generated by site-directed mutagenesis (Invitrogen) using oligonucleotides H502A and E18A (Table 1) following the manufacturer instructions. All constructs were verified by DNA sequencing.

2.2. Protein purification

NS5BΔ55 and its fusion derivatives were over-expressed and purified using the following protocols. *Escherichia coli* BL21(DE3)pLysS Rosetta cells (Novagen) were transformed with the construct of interest (pDest14-NS5BΔ55-FP or pDest14-NS5BΔ55). One colony was used to inoculate 5 ml of LB medium supplemented with ampicillin (100 μg/ml) and chloramphenicol (17 μg/ml), and grown overnight at 37 °C. This overnight preinoculum was used to inoculate 500–1000 ml of LB medium supplemented with the same antibiotics, and bacteria were allowed to grow at 37 °C until an OD at 600 nm of 0.8–1.0 was reached. The culture was supplemented with 2% absolute ethanol and incubated at 4 °C for 2 h before protein expression induction with 100 μM isopropyl 1-thio-β-D-galactopyranoside (IPTG) during 16–18 h at 17 °C. Bacteria were harvested by centrifugation and lysed, and the recombinant protein was bound to a Ni-NTA agarose affinity column (Invitrogen) in Tris buffer I (20 mM Tris–HCl pH 8.0, 0.5 M NaCl, 10% glycerol, 1% Triton X-100, 1 mM β-mercaptoethanol, 10 mM imidazol, 1 mM PMSF, 1 μg/μl DNaseI, 1 mg/mL lysozyme). The column was sequentially washed with Tris buffer II (20 mM Tris–HCl pH 7.0, 1 M NaCl, 10% glycerol, 1% Triton X-100, 1 mM β-mercaptoethanol) supplemented with 20 and 40 mM imidazol, and the resin-bound protein was eluted with Tris buffer II supplemented with 250 mM imidazol. Aliquots showing the purest and most concentrated protein were dialyzed against Tris buffer III (20 mM Tris–HCl pH 7.0, 1 M NaCl, 10% glycerol) and stored at 4 °C. All purification processes were followed by PAGE and Coomassie blue staining.

Citrine was over-expressed and purified by the following protocol. pRSET-citrine was used to transform *Escherichia coli* BL21(DE3)pLysS. Transformed cells were plated on LB-agar supplemented with ampicillin (100 μg/ml), incubated at room temperature for 2 days and then at 4 °C for 48 h. The most fluorescent colony was chosen to inoculate 10 ml of LB supplemented with ampicillin (100 μg/ml), and was grown overnight at 37 °C. A volume of 500 ml of LB supplemented with ampicillin (100 μg/ml) was inoculated with the overnight culture and grown at 37 °C until an OD at 600 nm of 0.5 was reached. Then the culture was induced with 0.5 mM IPTG during 2 h at room temperature. The protocol for citrine purification was identical to that used for NS5B derivatives, except that citrine was eluted from the Ni-NTA agarose with Tris buffer II supplemented with 50 mM imidazol.

2.3. RdRp activity assay

RdRp activity of NS5BΔ55-FP and non-fused-NS5BΔ55 were examined by GTP incorporation using a poly(C) template. 10 μl reaction mixtures contained 600 nM of NS5BΔ55 or 900 nM NS5BΔ55-FP, 0.5 μCi [α-^{32}P]GTP (PerkinElmer), 125 μM of unlabeled GTP (GE Healthcare), and 40 ng/μl of poly(C) template (Sigma Aldrich), in polymerase buffer (20 mM MOPS pH 7.25, 5 mM $MnCl_2$, 66 mM NaCl and 0.1 mM β-mercaptohetanol). Reactions were stopped after 1 h of incubation by adding 150 mM EDTA (final concentration). The reaction mixture was filtered throughout a DE81 paper (Whatman) to eliminate unincorporated radioactivity. The filters were then washed twice with nine ml of Na_2HPO_4, once with nine ml of H_2O and once with three ml of absolute ethanol, and were dried for 15 min at 55 °C. Incorporated radioactivity was measured by liquid scintillation counting.

Table 1
Oligonucleotides used in this study.

Name	Sequence (5′-3′)
ATTB1_NS5B	GGGGACAAGTTTGTACAAAAAAGCAGGCTTCTAAGGAGGTAGAACCATGAAATCAATGTCCTACACATGGACAGG
FPs_ATTB2	GGGGACCACTTTGTACAAGAAAGTCGGGTCCTAATGGTGATGGTGATGGTGCTTGTACAGCTCGTCCATGCCG
FPs_5G	TCTTCAACTGGGCAGTGAAGACCAAACTTAAACTCGGAGGTGGCGGAGGTGTGAGCAAGGGCGAGGAGCTGTTCA
NS5B_5G	TGAACAGCTCCTCGCCCTTGCTCACACCTCCGCCACCTCCGAGTTTAAGTTTGGTCTTCACTGCCCAGTTGAAGA
E18A-sense	CCATGCGCTGCGGAGGCAAGCAAGCTGCCC
E18A-antisense	GGGCAGCTTGCTTGCCTCCGCAGCGCATGG
H502A-sense	CGAGTCTGGAGAGCTCGGGCCAGGAGC
H502A-antisense	GCTCCTGGCCCGAGCTCTCCAGACTCG

The non-nucleoside inhibitor used in this study is the PF-254027, a derivative of the previously reported inhibitor PF-00868554 (Shi et al., 2009). PF-254027 was dissolved in dimethyl sulfoxide (DMSO) to a concentration of 10 mM and diluted to appropriate concentrations in buffer. For calculation of the IC_{50} for PF-254027, the RNA polymerase activity was measured as described above in the presence of increasing concentrations of the compound.

2.4. Electrophoretic mobility shift assay (EMSA)

A heteropolymeric RNA of 254 nt in length was labeled with [α-^{32}P]CTP (PerkinElmer) during its synthesis by *in vitro* transcription using the MAXIscript T7 Kit (Ambion). Labeled RNA was diluted in binding buffer (5 mM HEPES pH 7.6, 25 mM KCl, 2 mM $MgCl_2$, 3% glycerol, 200 mM NaCl, 0.02 mM DTT, 50 μg/ml tRNA) in the presence or absence of fusion protein (which ranged from 0.2 to 4 μM final concentration) to approximately 5000–10,000 cpm per reaction. The mixture was incubated for 10 min at 25 °C, and added to one volume of gel loading buffer (15% glycerol, 0.4% bromophenol blue). The mixture was then applied onto a native polyacrylamide gel (5% acrylamide–bisacrylamide (80:1), 4% glycerol, TBE 1×) previously pre-run at 20 mA for 30–60 min at room temperature. Electrophoresis was run for 2 h at 20 mA. Gel products were visualized by phosphorimaging (Typhoon, Molecular Dynamics).

2.5. Fluorescence spectroscopic and FRET analyses

NS5BΔ55-FP (NS5BΔ55-cyan and NS5BΔ55-citrine) were mixed and diluted at equimolar concentration (final concentration indicated in each experiment) in polymerase buffer (30 mM morpholinepropanesulfonic acid pH 7.0, 4.5 mM $Mg(CH_3COO)_2$) in the presence of variable NaCl or KCl concentration and molecules (unlabelled NS5BΔ55, antibodies, inhibitors) when indicated. For fluorescence spectroscopic analyses of NS5BΔ55 fused to cyan, the excitation wavelength (λ_{ex}) was set at 432 nm (excitation wavelength for cyan) to obtain fluorescence emission spectra from 460 to 600 nm. For fluorescence spectroscopic analyses of NS5BΔ55 fused to citrine, λ_{ex} was set at 460 nm (excitation wavelength for citrine) to obtain fluorescence emission from 500 to 600 nm. For FRET analyses, λ_{ex} was set at 432 nm to obtain fluorescence emission spectra from 460 to 600 nm. Spectra were recorded at 1200 nm/min using a 5 nm slit and the photomultiplier set at 900 V. If FRET conditions are optimal, then fluorescence increases at 530 nm (F530 citrine emission, FRET signal) while fluorescence at 478 nm decreases (F478 primary cyan emission) with an isosbestic wavelength at ~512 nm. As negative controls we subtracted the spectra obtained in the absence of any of those proteins and also in the presence of NS5BΔ55-citrine alone because citrine cross-excites slightly at 432 nm. Finally, the data were used to calculate a simple ratio of FRET (emission at 530 nm/emission at 478 nm). Fluorescence measurements were obtained in an LS-50B spectrofluorometer (PerkinElmer).

3. Results

3.1. Purification of fusion proteins

HCV NS5BΔ55-FP fusion proteins containing a 6x histidine tag at their C-terminal were over-expressed and purified to apparent homogeneity as judged by 10% SDS-PAGE and Coomassie blue staining following the protocol described in Section 2 (Fig. 1B). Main contaminants were eliminated during the 20 and 40 mM imidazol washing steps (Fig. 1B, lanes 3 and 4), and almost all the protein was recovered in the first 250 mM imidazol elution fractions (Fig. 1B, lanes 5 and 6). Similar results were obtained for the NS5BΔ55 purification (data not shown). The electrophoretic mobility of the purified NS5BΔ55 and NS5BΔ55-FP fusion proteins were compatible with their deduced molecular mass, 60.5 and 87.5 kDa, respectively (Fig. 1B, lanes 11, 13 and 14). The recombinant citrine was purified following the same protocol as for NS5BΔ55-FP fusion proteins, and analyzed by 12% SDS-PAGE (Fig. 1B). Contaminants were eliminated in the 20 mM washing step (Fig. 1B, lane 17) and most of the protein was recovered in the first elution at 50 mM imidazol (Fig. 1B, lane 18). The electrophoretic mobility of the purified citrine was compatible with its deduced molecular mass (27 kDa). Typical protein yield ranged from 2 to 10 mg.

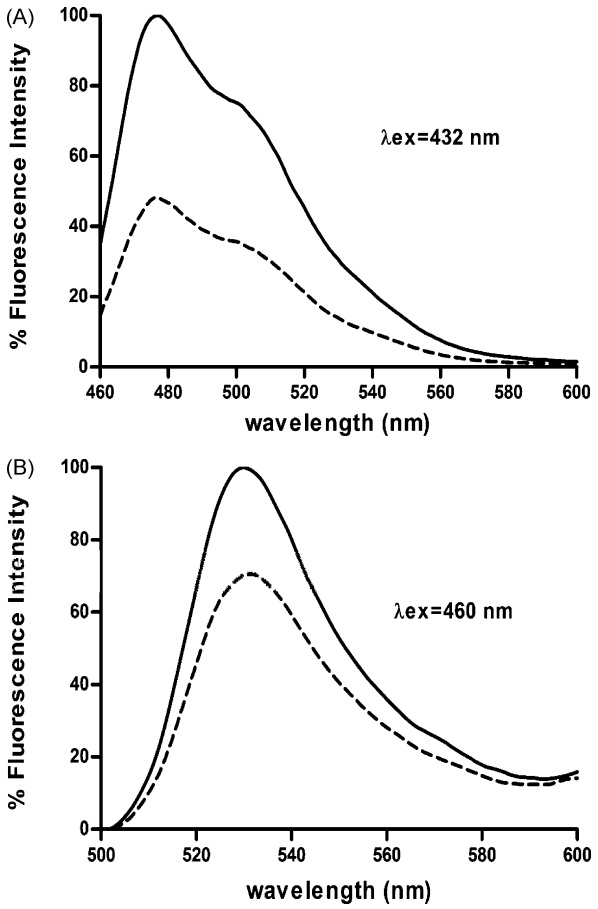

Fig. 2. Fluorescent properties of NS5B fused proteins. Representative spectra obtained for each protein as described in Section 2. (A) Emission spectra obtained for NS5B-cyan at 34 nM (dashed line) and 51 nM (continuous line) using the excitation wavelength for cyan (432 nm). (B) Emission spectra for NS5B-citrine at 34 nM (dashed line) and 51 nM (continuous line) using the excitation wavelength for citrine (460 nm).

3.2. Fluorescence properties of fusion proteins

To test if fluorescent proteins fused to HCV polymerase were properly folded, their fluorescence properties were analyzed. The emission spectra for NS5BΔ55-cyan showed a maximum peak at 478 nm and a minor peak at 496 nm, and the emission spectra for NS5BΔ55-citrine showed a maximum peak at 530 nm. Both spectra are as expected. Furthermore, emission intensity was dependent of protein concentration (Fig. 2A and B) making possible a precise control of protein concentration in the assay. As the emission and excitation spectra of both cyan and citrine slightly overlap, NS5BΔ55-citrine showed an emission peak at 530 nm when λ_{ex} was set at 432 nm (the λ_{ex} corresponding to cyan) even in the absence of NS5BΔ55-cyan (data not shown). This signal was con-

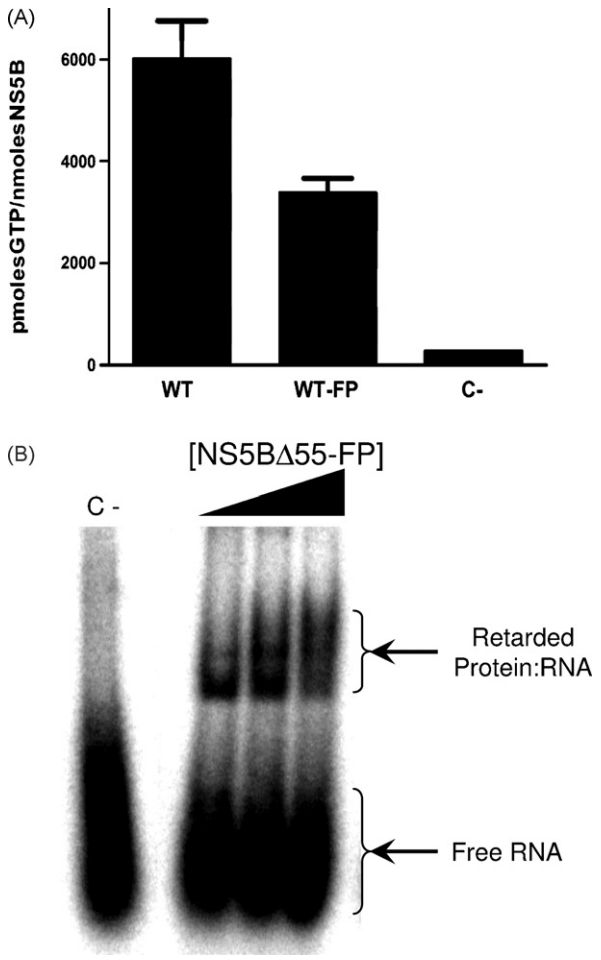

Fig. 3. Biochemical properties of fused proteins. (A) *De novo* polymerization activity by NS5BΔ55 and NS5BΔ55-FP polymerase. Reactions were performed as described in Section 2. The average value and standard error of the mean for at least three independent experiments are shown. C− is the negative control, without polymerase. (B) Electrophoretic mobility shift assay (EMSA). A 254 nt heteropolymeric RNA was used as probe. Free RNA probe and protein–RNA complexes are indicated. NS5BΔ55-FP concentrations assayed were 1, 2, and 4 μM.

sidered for each of the experiments, and the values obtained were subtracted in the calculations as negative controls.

3.3. Biochemical properties of fused proteins

The RdRp activity by *de novo* RNA polymerization determinations of NS5BΔ55-FP was compared to that of NS5BΔ55. NS5BΔ55 fused to the fluorescent protein was able to initiate polymerization by a *de novo* mechanism indicating that the C-terminal fusion of a fluorescent protein does not abolish RdRp activity (Fig. 3A). NS5BΔ55-FP specific activity value was lower than that showed by NS5BΔ55 indicating that fusion mutant is slightly less active for *de novo* RNA polymerization. RdRp activity was also analyzed in the presence of increasing concentrations of the non-nucleoside inhibitor PF-254027 and we obtained more than 60% reduction in *de novo* activity at 1 μM inhibitor concentration (data not shown).

To study if the binding of HCV polymerase to single-stranded RNA could be hindered by the presence of a fused FP in the NS5BΔ55 C-terminal, electrophoretic-mobility shift assays (EMSA) using a 254 nt heteropolymeric RNA were performed. Labeled RNA retarded in the presence of fused protein was detected (Fig. 3B). The intensity of the retarded product increased proportionally to the amount of protein added to the reaction. Therefore, and as expected because the fused protein showed RdRp activity, a FP fused to the NS5BΔ55 C-terminal did not hamper the binding of HCV polymerase to single-stranded RNA.

3.4. Quantification of NS5B oligomerization by FRET analyses

Once confirmed that the polymerase and the fluorescence protein domains were folded in a manner compatible with activity, the fluorescence-based system was used to analyze polymerase–polymerase interactions. To analyze polymerase–polymerase interactions, equimolar amounts of both NS5BΔ55-FP were mixed at different final NaCl concentrations, the sample excited at 432 nm and the emission spectra recorded from 460 to 600 nm. Results were obtained at different NaCl concentrations, and normalized against the isosbestic point at 512 nm. At NaCl concentrations of 200 mM or lower an emission peak at about 530 nm (F530 citrine emission), corresponding to FRET signal, was obtained (Fig. 4A). Furthermore, the fluorescence intensity of this FRET emission increased as the salt concentration decreased, whereas the intensity of the cyan at 478 nm (F478 primary cyan emission) decreased as the FRET signal increased. Similar results were obtained using a NS5BΔ21 mutant derived from HC-J4 strain (P Clemente-Casares and A Mas, unpublished results).

These results indicate that fluorescent protein interactions occur and in such a way to allow FRET emission. However, these data do not indicate the specificity of the interaction. To confirm that the obtained FRET was due to NS5B homoytpic interactions, a FRET experiment at 18.3 mM NaCl concentration was done by replacing the fusion protein NS5BΔ55-citrine with increasing concentrations of purified recombinant citrine (Fig. 4B). At this NaCl concentration we expect the maximum FRET signal. However, the obtained spectra totally overlapped with that for NS5BΔ55-cyan alone, in contrast to the spectrum obtained when both NS5BΔ55-FP proteins were equimolecularly mixed. FRET emission was not detected even at citrine concentration four times that of the NS5BΔ55-cyan counterpart.

To quantify the NS5B–NS5B oligomerization we calculated a simple ratio of FRET as the intensity of the FRET emission (F530 citrine emission) versus the intensity of primary emission (F478 primary cyan emission). This simple ratio of FRET was obtained at the different salt concentrations used in the experiments, and the data were fitted to a nonlinear regression curve (Fig. 4C). This curve allowed us to calculate the parameter termed FC_{50} (FRET concentration 50%) defined as the salt concentration at which the FRET value falls down to 50%, that is, the salt concentration in which at least the 50% of the NS5BΔ55-FP protein is in a dimeric, trimeric, or even oligomeric form, and the rest is monomeric. The obtained FC_{50} value for NaCl was 48.3 mM. This experiment was also made using increasing concentrations of KCl and the corresponding FC_{50} value was 73.2 mM.

3.5. Determination of protein–protein interaction inhibition

The procedure to quantify protein–protein interaction described above may be applied to analyze molecules that interfere with this protein–protein interaction. As a first approximation to explore this possibility, we competed the NS5B–NS5B interaction with a polyclonal antibody directed against NS5B. The reduction in the ratio of FRET was proportional to the concentration of the antibody, and the regression curve could be adjusted to a linear equation (Fig. 5A). An antibody concentration as low as 0.364 ng/μl was sufficient to diminish the ratio of FRET to 50%.

Then we performed competition experiments for the NS5BΔ55-cyan NS5BΔ55-citrine interaction using increasing concentrations of recombinant non-fused-NS5BΔ55 protein, purified as shown in Fig. 1B. Equimolar amounts of both fused proteins (50 nM

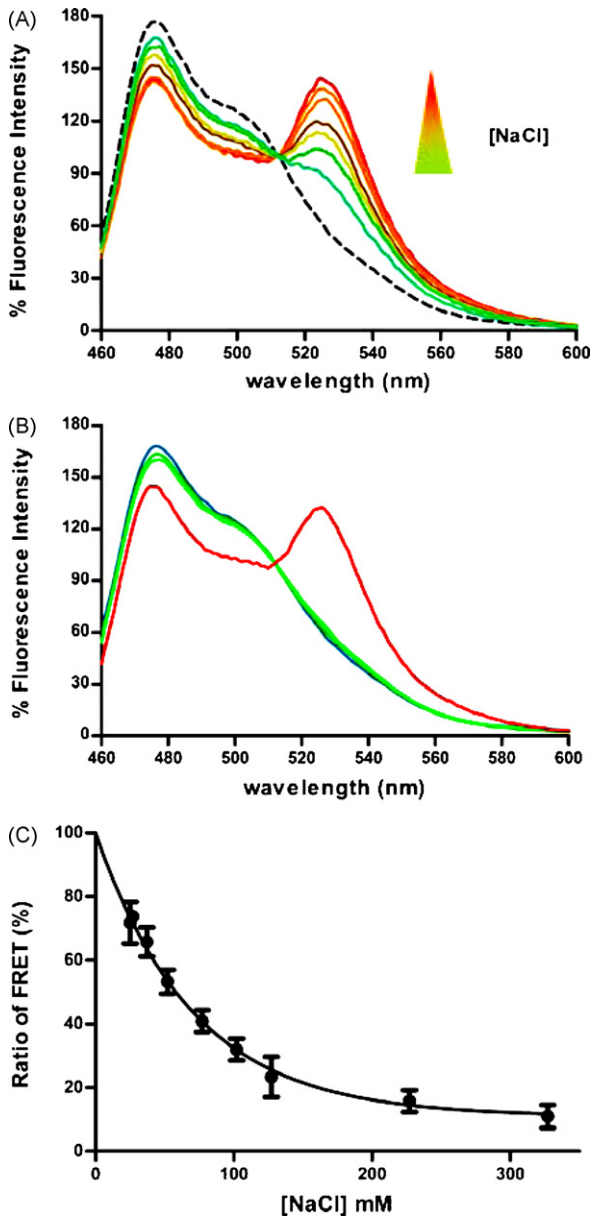

Fig. 4. FRET analyses. Representative spectra obtained for each protein and NaCl concentration are shown. (A) Emission spectra obtained from reactions where equimolar amounts of NS5B-cyan and NS5B-citrine were mixed at different NaCl concentration (from red to light green are 8.3, 18.3, 33.3, 58.3, 83.3, 108.3, and 208.3 mM). Emission spectrum of NS5B-cyan in the absence of NS5B-citrine was recorded as a negative control (dashed line). (B) Emission spectra obtained from reactions in which NS5B-cyan (50 nM) was mixed with increasing concentrations of recombinant citrine. The emission spectrum of the mixture NS5BΔ55-cyan and NS5BΔ55-citrine at 18.3 mM salt concentration is shown in orange as a positive control of FRET. Spectra obtained for NS5BΔ55-cyan in the presence of different concentrations of recombinant citrine (range of 50–200 nM) are shown in cyan, green and green forest. (C) Values of FRET concentration 50 (FC_{50}). Curve of efficiency of FRET (calculated as a simple ratio of FRET as described in Section 2) plotted in relation to NaCl concentration. The average value and standard error of the mean for at least six independent experiments are given. (For interpretation of the references to color in this figure legend, the reader is referred to the web version of the article.).

each) were incubated on ice for 10 min and then NS5BΔ55 was added at a final concentration ranging from 0 to 200 nM (Fig. 5B). FRET diminished until NS5BΔ55 was at the same concentration of the fused-NS5Bs (50 nM), and 30% of the FRET was lost when NS5BΔ55 was equimolecularly added to the reaction. Further increase of NS5BΔ55 (until 200 nM) did not lead to additional FRET reduction.

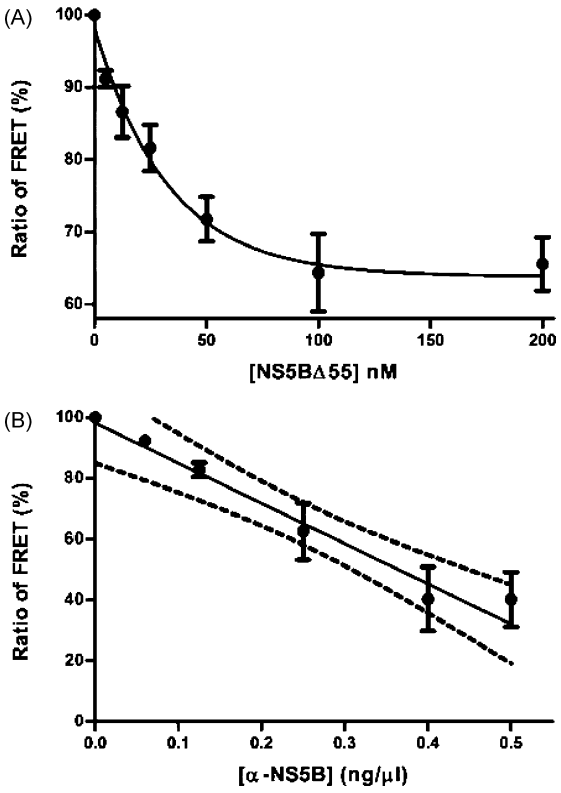

Fig. 5. Competition experiments. (A) Percentage of FRET ratio for the interaction of equimolecular amounts of NS5BΔ55-cyan and NS5BΔ55-citrine, in the presence of increasing concentrations (from 0.06 to 0.5 ng/μl) of a polyclonal antiboby directed against NS5B, and a NaCl concentration of 17.6 mM. 100% represent the point in the absence of the antibody. Dotted lines represent the 95% confidence interval. (B) Percentage of FRET ratio for the interaction of equimolar amounts of NS5BΔ55-cyan and NS5BΔ55-citrine in the presence of increasing concentrations of non-fused-NS5BΔ55. The fused proteins were used at a concentration of 50 nM. NS5BΔ55 was added at 0, 5, 12.5, 25, 50, 100, and 200 nM final concentrations. NaCl concentration was fixed at 20 mM. Results are the mean of at least three independent experiments.

Next, we performed experiments with point mutants E18A and H502A. These mutants have been previously reported as critical for NS5B–NS5B interactions (Qin et al., 2002). To test these positions with our fluorescence-based method, mutants in both fused proteins were generated, the fusion proteins were purified, and the FRET signal was analyzed. Results are shown in Fig. 6A. H502A mutant showed almost totally disappearance of FRET signal when both fusion proteins carried the mutation and about a 50% of FRET when only one of the fusion proteins was mutated and the other was WT. Unexpectedly, E18A mutant showed results similar to those obtained with WT proteins, with FRET values around 50% when mixed to H502A and 100% of FRET when mixed to WT NS5B. Interestingly, the FRET value when we mixed WT and the H502A mutant was around 50% independently of the fluorescent protein fused to each one (Fig. 6A).

Finally, we calculated the ratio of FRET at increasing NaCl concentrations in the absence and in the presence of the non-nucleoside analogue inhibitor (NNI) PF-254027 that binds to site 2 of the NS5B. Results are shown in Fig. 6B. NS5B–NS5B interaction was partially hampered at low NaCl concentrations, from 17.6 to 100 mM, whereas the curves from 100 to 300 mM were indistinguishable. The differences found at low NaCl concentrations were statistically significant, showing p values (Student's t-test) lower than 0.005 for NaCl concentration points of 17.6, 50, and 60 mM, and lower than 0.05 for 30 and 40 mM NaCl. Differences in NaCl curves observed between Figs. 4C and 6B were due to the presence of DMSO in the reaction buffer of the exper-

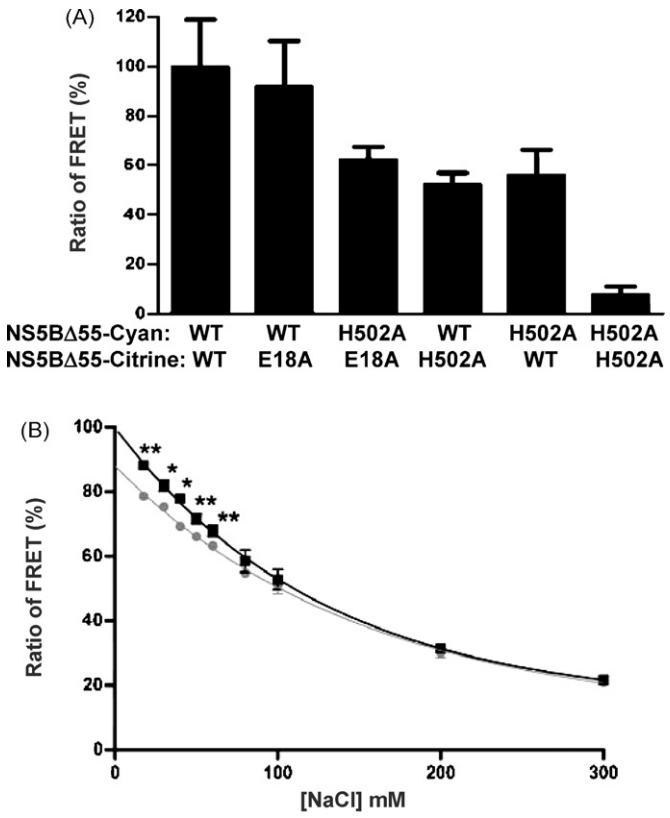

Fig. 6. Effect of point mutations and non-nucleoside inhibitor binding on NS5B self-interaction. (A) Mutations E18A and H502A were introduced either in NS5BΔ55-cyan and NS5BΔ55-citrine. Fusion proteins were over-expressed and purified and equimolar mixtures with NaCl concentration of 18.3 mM were assayed to calculate their corresponding ratios of FRET. The results are the average and the standard error of the mean of at least three independent experiments. (B) The ratio of FRET was calculated for equimolar mixtures of NS5BΔ55-cyan and NS5BΔ55-citrine at increasing salt concentrations either in the absence (black) or in the presence (gray) of 1 μM PF-254027. (*) Indicates $p < 0.05$, and (**) indicates $p < 0.005$ using a Student's *t*-test. The results are the average and the standard error of the mean of at least three independent experiments.

iments with NNI. Therefore, collectively our results document a sensitive FRET-based method that allows quantification of HCV polymerase–polymerase interactions. The method is valid to analyze the effect of NS5B mutants on polymerase oligomerization as well as the effect of molecules designed to block the interaction.

4. Discussion

In this study we document NS5B–NS5B interaction by using a new method based on FRET (Fig. 1A). We have analyzed the ratio of FRET at increasing salt concentrations and these data allowed us to define the FC_{50} parameter as the value corresponding to the salt concentration at which the ratio of FRET decreases by 50%. The FC_{50} values for NaCl and KCl are 48.3 and 73.2 mM, respectively (Fig. 4C). Since intracellular Na^+ and Cl^- concentrations in hepatocytes seems to be about 22 mM (Williams and Woodbury, 1971), and assuming the same concentration in the inner of the microvesicles where the HCV RC is located, NS5B protein would be shifted to an oligomeric state in the RC. Intracellular K^+ concentration is higher and FC_{50} for KCl was also higher. Obviously, the oligomerization state may also be influenced by the presence of other viral and probably host proteins, and the interactions among them in the RC (Quinkert et al., 2005; Shirota et al., 2002; Shimakami et al., 2004; Tu et al., 1999; Choi et al., 2004; Gao et al., 2004; Dimitrova et al., 2003; Hamamoto et al., 2005), in a phenomenon termed molecular crowding (Ellis, 2001).

Relationships among ionic strength, NS5B–NS5B interactions, and RNA polymerase activity remain controversial. Cramer and colleagues correlated oligomerization and ionic strength but they did not find any relation between oligomerization, and RNA polymerase activity measured as extension of a dinucleotide (Cramer et al., 2006). However, Heck and colleagues described the range of NaCl for the novo initiation synthesis by RNA polymerases from HCV genotypes 1 and 2 and in all cases high NaCl concentrations, above 100 mM for Con1 (genotype 1b) strain and above 50 mM for H77 (genotype 1a), J4 (genotype 1b) or J6 (genotype 2a) strains, were deleterious for RNA polymerase activity (Heck et al., 2008). Finally, mutants that disrupt NS5B–NS5B interactions were lethal for RdRp activity measured in primer extension assays (Qin et al., 2002). These results as a whole could be indicating that NS5B–NS5B interactions would be important at some but not all steps during HCV RNA polymerization process. Therefore, a simple and rapid method to analyze NS5B–NS5B interactions should be very useful for dissecting the NS5B catalytic cycle.

Functional polymerase–polymerase interactions during viral infection have been demonstrated for different RNA viruses including poliovirus (Hobson et al., 2001), Sendai virus (Smallwood et al., 2002), Rift Valley Fever virus (Zamoto-Niikura et al., 2009), norovirus (Högbom et al., 2009), nodavirus (Dye et al., 2005), tobacco mosaic virus (Goregaoker and Culver, 2003), and brome mosaic virus (O'Reilly et al., 1997). Recently, Spagnolo and colleagues have reported that poliovirus RNA polymerase is required both to catalyze polymerase reaction and to maintain the structure of the replication complex (Spagnolo et al., 2010). In fact, introduction of catalytically inactive polymerase into infected cells did not inactivate replication complexes, whereas introduction of protein–protein interaction mutants did (Spagnolo et al., 2010). HCV replicates its genetic material in RCs associated to ER membrane (Egger et al., 2002; Gosert et al., 2003). RNA and proteins involved in RNA replication are localized in these complexes, including the viral NS5B protein. The proportion of RNA to NS5B protein in these complexes has been calculated to be around 1–100 for positive-strand RNA and 1–1000 for the replication intermediate negative strand RNA (Quinkert et al., 2005). These data suggest that not all the NS5B proteins present in the HCV RC would necessarily be acting as RdRp, and some of them could play a structural role. NS5B–NS5B interactions have been demonstrated by gel filtration and yeast two hybrid (Wang et al., 2002), pull-down (Qin et al., 2002) and chemical cross-linking (Bellón-Echeverría I. et al, data not shown), although these methodological approaches do not allow accurate quantitative analyses. The small reduction in FRET we observe in the presence of NNI compared to more than 60% reduction in RdRp activity could be indicating that modest inhibition of the structural role of NS5B could provoke large effects in polymerase activity. Recent results point out this relationship between oligomerization and *de novo* activity (Chinnaswamy et al., 2010).

Amino acid positions E18 and H502 have already been involved in the oligomerization process, and NS5B carrying E18A or H502A mutations were inactive for both oligomerization and RdRp activities (Qin et al., 2002). However, these interactions were reported by non-quantitative methods, and the intensity of the contact might differ from one mutant to another. We show that mutant H502A is unable to oligomerize when NS5BΔ55-cyan and NS5BΔ55-citrine carrying both the mutation were assayed. This mutant rendered FRET values closed to cero in our fluorescence-based method (Fig. 6A). However, E18A mutant showed a behavior similar to WT. Interestingly, when we mixed H502A mutant with WT or E18A mutant, FRET values were reduced to approximately 50%. These results could be indicating either that we cannot detect interac-

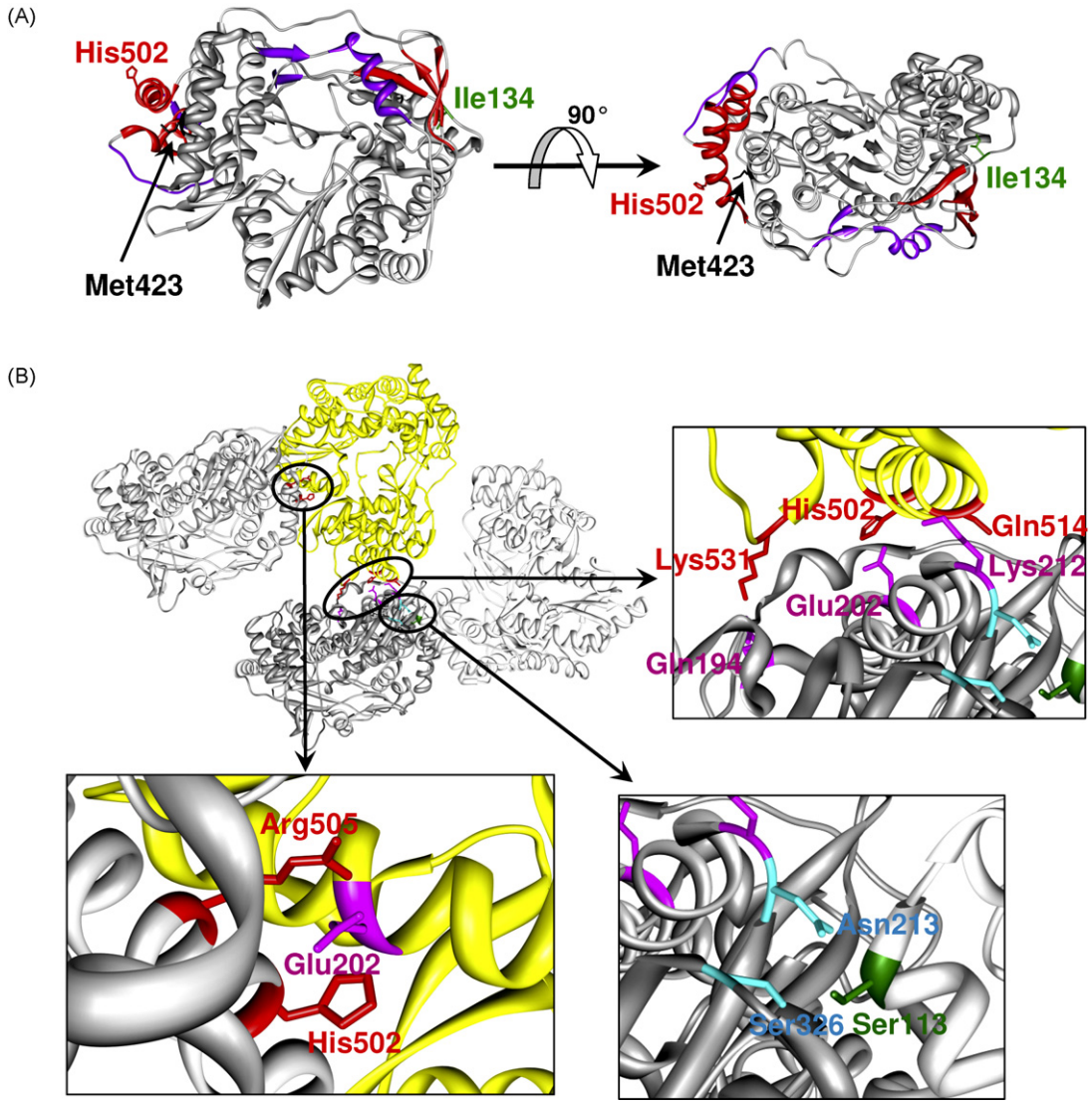

Fig. 7. Model of the NS5B interaction. (A) NS5B crystal structure (O'Farrell et al., 2003) showing in red and purple the regions involved in contact interfaces A and B, respectively as described in Wang et al., 2002. Residues Ile134, Met423 and His502 are highlighted in green, black and red, respectively. (B) NS5B crystal structure (PDB code 2ZKU) showing four molecules interacting by three different interfaces. The interfaces are detailed in boxes showing those residues that are located at a distance lower than 3 Å from one protein to the other. (For interpretation of the references to color in this figure legend, the reader is referred to the web version of the article.).

tions where E18 position is involved or that E18 position is not required in NS5B–NS5B interactions in our condition assays. In any case, these results clearly show that position H502 is involved in NS5B–NS5B interactions.

Some authors have proposed NS5B oligomerization as one of the processes inhibited by some anti-HCV NNIs based on crystallographic analyses (Love et al., 2003; Biswal et al., 2006). Wang et al. (2002) described two extensive interfaces from the packing of the NS5B molecules in the crystal lattice. These interfaces are represented in Fig. 7A, and are colored in red for interface A and in purple for interface B. These authors described that the helix αT and the loop connecting αT and αU, among other regions, are involved in these homotypic interactions. Interestingly, H502 is located in the helix αT. Moreover, Biswal and co-workers have also deposited a crystal structure (PDB code 2ZKU) showing four polymerases connected by three different interfaces, and the amino acid H502 is also involved in two of them (Fig. 7B). Wang et al. (2002) proposed a head-to-tail interaction between the thumb subdomain of one molecule and the fingers subdomain of the adjacent NS5B molecule. Results of FRET obtained with H502A mutants would be in accordance with the role played by this region of the NS5B.

Some NNI's bind to pockets located adjacent or even in the regions proposed to be involved in oligomerization. The inhibitor PF-254027, a derivative of the PF-00868554 (Shi et al., 2009), binds to the pocket defined by position M423 just below the helix αT (Fig. 7A). The reported mechanism of action for the thumb NNI inhibitors focused on the impediment of the dynamics between open and closed conformations needed for RNA synthesis properly (Biswal et al., 2006; Di Marco et al., 2005). We report in this study small but highly significant differences in NS5B homotypic interactions when this inhibitor is bound to the polymerase (Fig. 6B). It has been previously reported changes in the conformation of NS5B when a NNI of site two is bound (Biswal et al., 2006), and these changes could be in the basis of FRET differences. Resistance to NNI of site two is achieved mainly by mutation M423T that reduces the binding efficiency of the drug (Shi et al., 2009). However, changes in positions Ile134 and Asn110 far from the antiviral binding pocket are also selected (Shi et al., 2009). Mutations far from the inhibitor binding site could appear as compensatory mutations that increase the efficacy of the enzyme. Interestingly, residue Asn110 is closed (less than 4 Å) to helix αG where Ser113, that is part of one of the interaction interfaces showed in Fig. 7B, is located. Furthermore,

residue Ile134 is in closed contact (less than 3.5 Å) with the β4 strand (Fig. 7A) that is part of the region of the fingers domain involved in the interface A (Wang et al., 2002). Therefore, in the light of the structures showed in Fig. 7 we proposed that selected resistant mutations that appear far from the inhibitor binding site could modulate NS5B–NS5B contacts (Wang et al., 2002; Qin et al., 2002). Grouped together, these results open the possibility to explore new therapeutic interventions involving the inhibition of protein–protein interactions, as it has been already proposed for modulating signal transduction enzymes (Arkin and Whitty, 2009).

In conclusion, we describe a method that has allowed us to quantitatively analyze different aspects of HCV NS5B–NS5B interactions. Thus, we have described the FC_{50} parameter that indicates the most advantageous range of salt concentration optimum for NS5B–NS5B interaction. Finally, this method opens new perspectives for the study and characterization of compounds designed to block NS5B–NS5B interactions, and the quantitative analysis and characterization of their effects. Furthermore, fluorescence assays are easily miniaturized, and high-throughput screening of NS5B mutants and compounds in a pharmaceutical setting seems also possible.

Acknowledgements

We thank Bruno Canard for providing pDest14-NS5BΔ55 and Juan Llopis for sharing pcDNA3-cyan and pRSET-citrine. Bruno Canard is also acknowledged for critical help in over-expression and purification of recombinant proteins. PF-254027 was a kindly gift of Helen Lavender (Pfizer, Sandwich UK). The authors also thank Juan Llopis for comments and suggestions, and Rosario Sabariegos, Ricardo Sánchez, and Esteban Domingo for critical review of the manuscript. This work was supported by Fondo de Investigaciones Sanitarias [grant number PI060584], Ministerio de Ciencia e Innovación [grant number HF2007-0015] and Consejería de Educación de Castilla La Mancha [grant number PAI07-0011-3655]. I.B.E. and A.J.L.J. were supported by predoctoral fellowships from Fundación para la Investigación Sanitaria de Castilla-La Mancha [grant numbers MOV-2006_JI/06 and MOV-2008_JI/1]. P.C.C. and A.M. were supported by a "Sara Borrell" contract from Fondo de Investigaciones Sanitarias and a Ramon y Cajal contract (Ministerio de Ciencia e Innovación cofinanced with FEDER funds), respectively. The funders had no role in study design, data collection and analysis, decision to publish, or preparation of the manuscript.

References

Allison, A.C., 1971. The role of membranes in the replication of animal viruses. Int. Rev. Exp. Pathol. 10, 181–242.
Arkin, M.R., Whitty, A., 2009. The road less travelled: modulating signal transduction enzymes by inhibiting their protein–protein interactions. Curr. Opin. Chem. Biol. 13, 284–290.
Behrens, S.E., Tomei, L., De Francesco, R., 1996. Identification and properties of the RNA-dependent RNA polymerase of hepatitis C virus. EMBO J. 15, 12–22.
Biswal, B.K., Wang, M., Cherney, M.M., Chan, L., Yannopoulos, C.G., Bilimoria, D., Bedard, J., James, M.N., 2006. Non-nucleoside inhibitors binding to hepatitis C virus NS5B polymerase reveal a novel mechanism of inhibition. J. Mol. Biol. 361, 33–45.
Caliguiri, L.A., Tamm, I., 1969. Membranous structures associated with translation and transcription of poliovirus RNA. Science 166, 885–886.
Care, S., Bignon, C., Pelissier, M.C., Blanc, E., Canard, B., Coutard, B., 2008. The translation of recombinant proteins in *E. coli* can be improved by in silico generating and screening random libraries of a −70/+96 mRNA region with respect to the translation initiation codon. Nucleic Acids Res. 36, e6.
Carette, J.E., van Lent, J., MacFarlane, S.A., Wellink, J., van Kammen, A., 2002. Cowpea mosaic virus 32- and 60-kilodalton replication proteins target and change the morphology of endoplasmic reticulum membranes. J. Virol. 76, 6293–6301.
Chinnaswamy, S., Murali, A., Li, P., Fujisaki, K., Kao, C.C., 2010. Regulation of de novo initiated RNA synthesis in the hepatitis C virus RNA dependent RNA polymerase by intermolecular interactions. J Virol. 2010 Apr 7. [Epub ahead of print], doi:10.1128/JVI.02446-09.
Choi, Y.W., Tan, Y.J., Lim, S.G., Hong, W., Goh, P.Y., 2004. Proteomic approach identifies HSP27 as an interacting partner of the hepatitis C virus NS5A protein. Biochem. Biophys. Res. Commun. 318, 514–519.
Cramer, J., Jaeger, J., Restle, T., 2006. Biochemical and pre-steady-state kinetic characterization of the hepatitis C virus RNA polymerase (NS5Bdelta21, HC-J4). Biochemistry 45, 3610–3619.
De Francesco, R., Migliaccio, G., 2005. Challenges and successes in developing new therapies for hepatitis C. Nature 436, 953–960.
Denison, M.R., 2008. Seeking membranes: positive-strand RNA virus replication complexes. PLoS Biol. 6, e270, doi:10.1371/journal.pbio.0060270.
Di Marco, S., Volpari, C., Tomei, L., Altamura, S., Harper, S., Narjes, F., Koch, U., Rowley, M., De Francesco, R., Migliaccio, G., Carfí, A., 2005. Interdomain communication in hepatitis C virus polymerase abolished by small molecule inhibitors bound to a novel allosteric site. J. Biol. Chem. 280, 29765–29770.
Dimitrova, M., Imbert, I., Kieny, M.P., Schuster, C., 2003. Protein–protein interactions between hepatitis c virus nonstructural proteins. J. Virol. 77, 5401–5414.
Dye, B.T., Miller, D.J., Ahlquist, P., 2005. In vivo self-interaction of nodavirus RNA replicase protein a revealed by fluorescence resonance energy transfer. J. Virol. 79, 8909–8919.
Egger, D., Wölk, B., Gosert, R., Bianchi, L., Blum, H.E., Moradpour, D., Bienz, K., 2002. Expression of hepatitis C virus proteins induces distinct membrane alterations including a candidate viral replication complex. J. Virol. 76, 5974–5984.
Ellis, R.J., 2001. Macromolecular crowding: obvious but underappreciated. Trends Biochem. Sci. 26, 597–604.
Förster, T., 1965. Delocalized Excitation and Excitation Transfer. Academic Press, Inc., New York, NY, pp. 93–137.
Gao, L., Aizaki, H., He, J.W., Lai, M.M., 2004. Interactions between viral nonstructural proteins and host protein hVAP-33 mediate the formation of hepatitis C virus RNA replication complex on lipid raft. J. Virol. 78, 3480–3488.
Goregaoker, S.P., Culver, J.N., 2003. Oligomerization and activity of the helicase domain of the tobacco mosaic virus 126- and 183-kilodalton replicase proteins. J. Virol. 77, 3549–3556.
Gosert, R., Kanjanahaluethai, A., Egger, D., Bienz, K., Baker, S.C., 2002. RNA replication of mouse hepatitis virus takes place at double-membrane vesicles. J. Virol. 76, 3697–3708.
Gosert, R., Egger, D., Lohmann, V., Bartenschlager, R., Blum, H.E., Bienz, K., Moradpour, D., 2003. Identification of the hepatitis C virus RNA replication complex in Huh-7 cells harboring subgenomic replicons. J. Virol. 77, 5487–5492.
Gu, B., Gutshall, L.L., Maley, D., Pruss, C.M., Nguyen, T.T., Silverman, C.L., Lin-Goerke, J., Khandekar, S., Liu, C., Baker, A.E., Casper, D.J., Sarisky, R.T., 2004. Mapping cooperative activity of the hepatitis C virus RNA-dependent RNA polymerase using genotype 1a-1b chimeras. Biochem. Biophys. Res. Commun. 313, 343–350.
Hamamoto, I., Nishimura, Y., Okamoto, T., Aizaki, H., Liu, M., Mori, Y., Abe, T., Suzuki, T., Lai, M.M., Miyamura, T., Moriishi, K., Matsuura, Y., 2005. Human VAP-B is involved in hepatitis C virus replication through interaction with NS5A and NS5B. J. Virol. 79, 13473–13482.
Hatta, T., Francki, R.I.B., 1981. Cytopathic structures associated with tonoplasts of plant cells infected with cucumber mosaic and tomato aspermy viruses. J. Gen. Virol. 53, 343–346.
Heck, J.A., Lam, A.M., Narayanan, N., Frick, D.N., 2008. Effects of mutagenic and chain-terminating nucleotide analogs on enzymes isolated from hepatitis C virus strains of various genotypes. Antimicrob. Agents Chemother. 52, 1901–1911.
Hobson, S.D., Rosenblum, E.S., Richards, O.C., Richmond, K., Kirkegaard, K., Schultz, S.C., 2001. Oligomeric structures of poliovirus polymerase are important for function. EMBO J. 20, 1153–1163.
Högbom, M., Jäger, K., Robel, I., Unge, T., Rohayem, J., 2009. The active form of the norovirus RNA-dependent RNA polymerase is a homodimer with cooperative activity. J. Gen. Virol. 90, 281–291.
Kim, K.S., 1977. An ultrastructural study of inclusions and disease in plant cells infected by cowpea chlorotic mottle virus. J. Gen. Virol. 35, 535–543.
Kolykhalov, A.A., Mihalik, K., Feinstone, S.M., Rice, C.M., 2000. Hepatitis C virus-encoded enzymatic activities and conserved RNA elements in the 3′ nontranslated region are essential for virus replication in vivo. J. Virol. 74, 2046–2051.
Kopek, B.G., Perkins, G., Miller, D.J., Ellisman, M.H., Ahlquist, P., 2007. Three-dimensional analysis of a viral RNA replication complex reveals a virus-induced mini-organelle. PLoS Biol. 5, e220, doi:10.1371/journal.pbio.0050220.
Kujala, P., Ikäheimonen, A., Ehsani, N., Vihinen, H., Auvinen, P., Kääriäinen, L., 2001. Biogenesis of the Semliki Forest virus RNA replication complex. J. Virol. 75, 3873–3884.
Lavanchy, D., 2008. Chronic viral hepatitis as a public health issue in the world. Best Pract. Res. Clin. Gastroenterol. 22, 991–1008.
Lohmann, V., Körner, F., Herian, U., Bartenschlager, R., 1997. Biochemical properties of hepatitis C virus NS5B RNA-dependent RNA polymerase and identification of amino acid sequence motifs essential for enzymatic activity. J. Virol. 71, 8416–8428.
Love, R.A., Parge, H.E., Yu, X., Hickey, M.J., Diehl, W., Gao, J., Wriggers, H., Ekker, A., Wang, L., Thomson, J.A., Dragovich, P.S., Furhman, S.A., 2003. Crystallographic identification of a noncompetitive inhibitor binding site on the hepatitis C virus NS5B RNA polymerase enzyme. J. Virol. 77, 7575–7581.
Lyle, J.M., Bullitt, E., Bienz, K., Kirkegaard, K., 2002. Visualization and functional analysis of RNA-dependent RNA polymerase lattices. Science 96, 2218–2222.
Magliano, D., Marshall, J.A., Bowden, D.S., Vardaxis, N., Meanger, J., Lee, J.Y., 1998. Rubella virus replication complexes are virus-modified lysosomes. Virology 240, 57–63.

Miller, S., Krijnse-Locker, J., 2008. Modification of intracellular membrane structures for virus replication. Nat. Rev. Microbiol. 6, 363–374.
Miyawaki, A., Tsien, R.Y., 2000. Monitoring protein conformations and interactions by fluorescence resonance energy transfer between mutants of green fluorescent protein. Methods Enzymol. 327, 472–500.
O'Farrell, D., Trowbridge, R., Rowlands, D., Jäger, J., 2003. Substrate complexes of hepatitis C virus RNA polymerase (HC-J4): structural evidence for nucleotide import and de-novo initiation. J. Mol. Biol. 326, 1025–1103.
O'Reilly, E.K., Paul, J.D., Kao, C.C., 1997. Analysis of the interaction of viral RNA replication proteins by using the yeast two-hybrid assay. J. Virol. 71, 7526–7532.
Pata, J.D., Schultz, S.C., Kirkegaard, K., 1995. Functional oligomerization of poliovirus RNA-dependent RNA polymerase. RNA 1, 466–477.
Patterson, G.H., Piston, D.W., Barisas, B.G., 2000. Förster distances between green fluorescent protein pairs. Anal. Biochem. 284, 438–440.
Prod'homme, D., Le Panse, S., Drugeon, G., Jupin, I., 2001. Detection and subcellular localization of the turnip yellow mosaic virus 66K replication protein in infected cells. Virology 281, 88–101.
Qin, W., Yamashita, T., Shirota, Y., Lin, Y., Wei, W., Murakami, S., 2001. Mutational analysis of the structure and functions of hepatitis C virus RNA-dependent RNA polymerase. Hepatology 33, 728–737.
Qin, W., Luo, H., Nomura, T., Hayashi, N., Yamashita, T., Murakami, S., 2002. Oligomeric interaction of hepatitis C virus NS5B is critical for catalytic activity of RNA-dependent RNA polymerase. J. Biol. Chem. 277, 2132–2137.
Quinkert, D., Bartenschlager, R., Lohmann, V., 2005. Quantitative analysis of the hepatitis C virus replication complex. J. Virol. 79, 13594–13605.
Ralph, R.K., Bullivant, S., Wojcik, S.J., 1971. Cytoplasmic membranes, a possible site of tobacco mosaic virus RNA replication. Virology 43, 713–716.
Schwartz, M., Chen, J., Janda, M., Sullivan, M., den Boon, J., Ahlquist, P., 2002. A positive-strand RNA virus replication complex parallels form and function of retrovirus capsids. Mol. Cell. 9, 505–514.
Shi, S.T., Herlihy, K.J., Graham, J.P., Nonomiya, J., Rahavendran, S.V., Skor, H., Irvine, R., Binford, S., Tatlock, J., Li, H., Gonzalez, J., Linton, A., Patick, A.K., Lewis, C., 2009. Preclinical characterization of PF-00868554, a potent nonnucleoside inhibitor of the hepatitis C virus RNA-dependent RNA polymerase. Antimicrob. Agents Chemother. 53, 2544–2552.
Shimakami, T., Hijikata, M., Luo, H., Ma, Y.Y., Kaneko, S., Shimotohno, K., Muralami, S., 2004. Effect of interaction between hepatitis C virus NS5A and NS5B on hepatitis C virus RNA replication with the hepatitis C virus replicon. J. Virol. 78, 2738–2748.
Shirota, Y., Luo, H., Qin, W., Kaneko, S., Yamashita, T., Kobayashi, K., Murakami, S., 2002. Hepatitis C virus (HCV) NS5A binds RNA-dependent RNA polymerase (RdRP) NS5B and modulates RNA-dependent RNA polymerase activity. J. Biol. Chem. 277, 11149–11155.
Smallwood, S., Cevik, B., Moyer, S.A., 2002. Intragenic complementation and oligomerization of the L subunit of the sendai virus RNA polymerase. Virology 20, 235–245.
Spagnolo, J.F., Rossignol, E., Bullitt, E., Kirkegaard, K., 2010. Enzymatic and nonenzymatic functions of viral RNA-dependent RNA polymerases within oligomeric arrays. RNA 16, 382–393.
Sreevalsan, T., 1970. Association of viral ribonucleic acid with cellular membranes in chick embryo cells infected with Sindbis virus. J. Virol. 6, 438–444.
Taylor, M.P., Kirkegaard, K., 2008. Potential subversion of autophagosomal pathway by picornaviruses. Autophagy 4, 286–289.
Tu, H., Gao, L., Shi, S.T., Taylor, D.R., Yang, T., Mircheff, A.K., Wen, Y., Gorbalenya, A.E., Hwang, S.B., Lai, M.M., 1999. Hepatitis C virus RNA polymerase and NS5A complex with a SNARE-like protein. Virology 263, 30–41.
Wang, Q.M., Hockman, M.A., Staschke, K., Johnson, R.B., Case, K.A., Lu, J., Parsons, S., Zhang, F., Rathnachalam, R., Kirkegaard, K., Colacino, J.M., 2002. Oligomerization and cooperative RNA synthesis activity of hepatitis C virus RNA-dependent RNA polymerase. J. Virol. 76, 3865–3872.
Wang, M., Ng, K.K.S., Cherney, M.M., Chan, L., Yannopoulos, C.G., Bedard, J., Morin, N., Nguyen-Ba, N., Alaoui-Ismaili, M.H., Bethell, R.C., James, M.N., 2003. Non-nucleoside analogue inhibitors bind to an allosteric site on HCV NS5B polymerase. Crystal structures and mechanism of inhibition. J. Biol. Chem. 278, 9489–9495.
Webster, D.P., Klenerman, P., Collier, J., Jeffery, K.J., 2009. Development of novel treatments for hepatitis C. Lancet Infect. Dis. 9, 108–117.
Welsch, S., Miller, S., Romero-Brey, I., Merz, A., Bleck, C.K., Walther, P., Fuller, S.D., Antony, C., Krijnse-Locker, J., Bartenschlager, R., 2009. Composition and three-dimensional architecture of the dengue virus replication and assembly sites. Cell Host Microb. 5, 365–375.
Westaway, E., Mackenzie, J., Kenney, M., Jones, M., Khromykh, A., 1997. Ultrastructure of Kunjin virus-infected cells: colocalization of NS1 and NS3 with double-stranded RNA, and of NS2B with NS3, in virus-induced membrane structures. J. Virol. 71, 6650–6661.
Williams, J.A., Woodbury, D.M., 1971. Determination of extracellular and intracellular electrolytes in rat liver in vivo. J. Physiol. 212, 85–99.
Zacharias, D.A., Violin, J.D., Newton, A.C., Tsien, R.Y., 2002. Partitioning of lipid-modified monomeric GFPs into membrane microdomains of live cells. Science 296, 913–916.
Zamoto-Niikura, A., Terasaki, K., Ikegami, T., Peters, C.J., Makino, S., 2009. Rift valley fever virus L protein forms a biologically active oligomer. J. Virol. 83, 12779–12789.